Stability and kinetics of step motion on crystal surfaces

Fong Liu[1] and Horia Metiu[2]
[1]*Institute for Theoretical Physics and Center for Quantized Electronic Structures, University of California, Santa Barbara, California 93106*
[2]*Department of Chemistry, University of California, Santa Barbara, California 93106*
(Received 19 November 1993)

The kinetics of monoatomic steps in diffusion-controlled crystal growth and evaporation processes are investigated analytically using a Green's function approach. Integro-differential equations of motion for the steps are derived; a systematic linear stability analysis is carried out treating simultaneously perturbations both along and perpendicular to the steps. Morphological fluctuations of steadily moving steps in response to ambient thermodynamic noises are also studied within a general Langevin formalism. Finally, a phase field model is developed to investigate the time-dependent, collective motion of steps. An application of the model to a finite step train recovers a variety of kinetic behaviors such as the bunching and spreading of steps.

PACS number(s): 05.40.+j, 61.50.Cj, 68.35.Ja

I. INTRODUCTION

The kinetics of atomic steps play a central role in the growth of singular crystal surfaces from vapor, liquid, and solid phases, in a wide variety of materials. Step motion is also a predominant elementary process governing such macroscopic changes of crystal surface topography as dissolution, faceting, etching, and coarsening. Numerous investigations, both theoretical and experimental, have been devoted to understand the morphology and dynamics of atomic steps. Recent resurgence of interests in step dynamics is largely stimulated by the development of crystal growth methods with atomic precision, and by the advances in high-resolution microscopies.

This paper addresses several theoretical aspects of the kinetics of diffusively coupled steps. Our investigation is based upon the classical model of step kinetics developed by Burton, Cabrera, and Frank (BCF) [1]. The ideal BCF model visualizes the singular crystal surface as consisting of closely packed terraces separated by elementary steps. Growth of crystal then proceeds through the lateral progression of these steps by incorporating diffusing adatoms from the terraces. The BCF model, supplemented with later modifications and extensions, has been extensively investigated and remains the most mathematically well-posed model of crystal growth by step flow dynamics. Although we restrict ourselves to the behavior of monoatomic steps governed by surface diffusion, and to situations where other assumptions of the BCF model are valid, we hope that this study can stimulate progress in elucidating the role of steps (not necessarily elementary) under other growth conditions, e.g., the growth of crystal by molecular epitaxy, or the ledge growth by volume diffusion in solid-solid phase transformations.

One central question in step kinetics concerns the morphological stability of step patterns. Steps are seldom seen to be equally spaced. It is also observed that fluctuations in the distance between steps can often lead to the bunching of them into multistep bands. Furthermore, meandering of the steps along the step direction on scales much greater than molecular length scale is commonplace. Bales and Zangwill [2] recently pointed out that, in addition to the effect of equilibrium fluctuations, a diffusive instability can contribute to the meandering of steps under growth situations. To address the stability issue, linear stability analyses, treating separately fluctuations in the spacing between adjacent steps and that along the step direction, have been carried out. Nevertheless, two popular approximations are often adopted. First, when considering perturbations in the step spacings, it is commonly assumed that the velocity of a step only depends upon the width of its two adjacent terraces. Second, in treating fluctuations along the steps, and in studying the motion of steps in general, a quasistatic approximation is used by assuming sufficient slow motion of steps. While these approximations are believed to be good for widely separated steps and under small driving forces, a fully time-dependent analysis is warranted in the opposite situations. As emphasized by Ghez and Iyer [3], such situations may arise particularly in certain epitaxy experiments where the so-called fast steps are encountered and where nearby steps are strongly coupled by their overlapping diffusion fields. Linear stability analysis which takes account of the overlap of diffusion fields has recently been carried out numerically [4,5]. In this paper, the step flow problem is formulated using a Green's function approach. Time-dependent integro-differential equations of motion for the step positions are derived, from which a systematic linear stability analysis is carried out. This formulation allows a simultaneous treatment of generic perturbations both along step extension and in the step spacings. The validity of the quasistatic approximation and the effect of the overlap of terrace diffusion fields are also examined. These works are discussed in Secs. II–IV. Section V analyzes the effect of asymmetric attachment kinetics on the linear stability of infinite step trains, under both growth and evaporation

situations.

In Sec. VI, we discuss the morphological fluctuations of steps during nonequilibrium growth using a Langevin formalism. In this formalism, local thermodynamical noises on the terraces and on the steps are assumed to be the sole sources of fluctuations which get amplified dynamically during growth and lead to the roughness of steps. We show that this method consistently recovers the equilibrium fluctuations. While step roughness in equilibrium does not depend on step spacing, we found that the diffusive coupling of steps in motion during growth gives rise to a correlation between fluctuations on different steps.

While stability analysis gives important information with regard to the role of step kinetics in crystal growth, more insights can only be provided by detailed investigations of the temporal development of step configurations. It is crucially required, for example, to interpret *in situ* experimental observations. In Sec. VII, we develop a phase field approach to study the time-dependent motion of finite and generically nonequidistant step trains. This method is numerically efficient, easily adaptable to two dimensions, compatible with shape fluctuations along the step extension, and able to simulate complicated time-dependent morphology of step patterns.

II. THE BCF MODEL

Consider the mathematical formulation of the original BCF model, for a close-packed crystal surface below its roughening transition temperature, growing from a supersaturated mother medium. We concentrate on the layer-by-layer growth mechanism characterized by the diffusion-controlled propagation of monoatomic steps, and neglect entirely the effect of two-dimensional island nucleation, under the assumption of small supersaturations. For concreteness, it is further assumed that the growth units are incorporated to the steps through diffusion along the terraces only. Although this mode of building growth units is predominant in vapor and solution growth, the alternative mode of depositing growth units directly from the bulk mother medium is important in certain solution growth environments and particularly in solid-solid phase transformations. The BCF formulation is equally applicable to crystal evaporation and dissolution processes.

In the BCF model, transport of adatoms on the terraces proceeds through surface diffusion according to

$$\frac{\partial c}{\partial t}=D\nabla^2 c-\frac{c-c_\infty}{\tau_s}\ , \tag{2.1}$$

where $c(\mathbf{r},t)$ is the adatom density, τ_s is the mean lifetime of adatom on the terraces before evaporating into the vapor, c_∞ is the adatom density far away from the steps, and D is a diffusion coefficient assumed isotropic over all terraces. In the present macroscopic description, steps are regarded as mathematically sharp dividing lines between terraces. A crucial assumption, inherent in most continuum treatments, demands that the monoatomic steps are molecularly rough with numerous kink excitations so as to behave as ideal line sinks for growth units. The condition of molecular roughness of steps is also a prerequisite for us to safely neglect lateral diffusion of adatoms along the steps, and to assume isotropic advancement of steps. A lower kink density hence smoother steps often implies stronger effect of attachment kinetics and more pronounced anisotropy in step motion and morphology. These and other assumptions of the BCF approach must be carefully examined when applying the original model to experiments, particularly to such nonconventional situations as molecular beam epitaxy [3] at low temperatures.

Relevant microscopic details of the atomic processes near the steps are reflected in the boundary conditions on the sharp steps. First, conservation of materials requires that the normal velocity of a step satisfies

$$c_r v_n=D[(\nabla c)_+-(\nabla c)_-]\cdot\mathbf{n}\ , \tag{2.2}$$

where c_r is the change of atomic density in the area swept by the moving step, $\mathbf{n}$ is the unit normal to the step, and $(\nabla c)_\pm$ are gradients computed on the two sides of a step, respectively. Secondly, another boundary condition relates the density of adatoms at the step to its local equilibrium value, taking into account the curvature correction via the Gibbs-Thompson relation:

$$c_{\text{step}}=c_0\left[1+\frac{\gamma\Omega}{k_B T}\kappa\right]\ , \tag{2.3}$$

where c_0 is the adatom density for a straight step in equilibrium, γ is the isotropic line tension of the step, Ω is the atomic area of the solid, and κ is the step curvature. The density of adatoms far away from the steps is maintained above the equilibrium density at $c_\infty > c_0$ through supersaturation, providing the driving force for step propagation. We have neglected the effect of crystalline anisotropy and also temporarily ignored the elevation of adatom density at the steps due to attachment kinetics. Equations (2.1)–(2.3) complete the description of the *symmetric* BCF model for crystal growth by the step flow mechanism, where atomic processes on both sides of a step contribute equivalently to step progression. The corresponding *asymmetric* version of the model, accounting for nonequivalent attachment kinetics as first discussed by Schwoebel and Shipsey [6], will be considered in Sec. V.

Multiple length scales are involved in the current problem, whose relative ratios characterize different growth regimes and determine the validity of various approximations. With the assumption of mathematically sharp steps, the continuum model is understood to apply on length scales much longer than the microscopic capillary length d_0 (to be defined below). Among the relevant macroscopic length scales, the mean adatom diffusion length on the terraces is given by $x_s\equiv\sqrt{D\tau_s}$, and the typical step spacing is denoted by λ. Another quantity $l=2D/v$ with dimensionality of length can be conveniently introduced as an alternative measure of the speed of step motion. Defining a quantity

$$u(\mathbf{r},t)=\frac{c_\infty-c(\mathbf{r},t)}{c_r} \tag{2.4}$$

and measuring time in units of τ_s, length in units of x_s, and velocity in units of $\sqrt{D/\tau_s}$, the equations of motion can be written in the dimensionless form

$$\frac{\partial u}{\partial t}=\nabla^2 u-u \ , \tag{2.5}$$

$$v_n=-[(\nabla u)_+-(\nabla u)_-]\cdot\mathbf{n} \ , \tag{2.6}$$

$$u_{\text{step}}=\Delta-d_0\kappa \ , \tag{2.7}$$

where $\Delta=(c_\infty-c_0)/c_r$ is the dimensionless supersaturation and $d_0=\gamma\Omega c_0/(k_B T c_r x_s)$ is the dimensionless capillary length. The problem defined by (2.5)–(2.7) resembles closely the problem of solidification [7], in spite of the extra homogeneous term $-u$ on the right-hand side of (2.5).

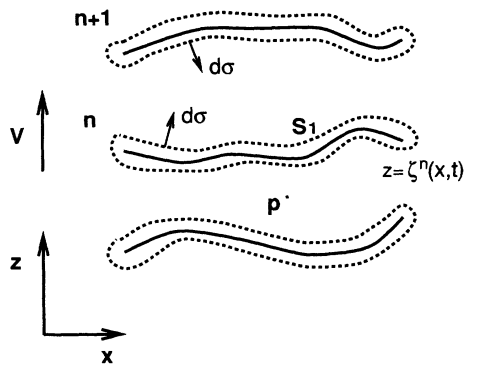

FIG. 1. Schematic representation of a train of steps moving in the z direction.

III. EQUATION OF MOTION FOR THE STEPS

The moving boundary problem (2.5)–(2.7) belongs to a general category of problems known as the Stefan problem, and is strongly nonlinear in character. One must solve a diffusionlike equation subject to boundary conditions which themselves depend upon the solution of the same diffusion equation. Complete analytic treatment of the entire problem in 2-space and 1-time dimensions is difficult. Even the linear stability analysis has only been carried out for synchronously moving equidistant steps, under quasistatic approximations. Studies of time-dependent step motion, particularly for nonequidistant steps, are even more limited. Fortunately, progress can be made analytically by reformulating the full (2+1)-dimensional problem in terms of a closed set of integro-differential equations for the positions of the steps. This boundary integral method, using Green's functions, was first put forward by Langer and Turski in their study of directional solidification fronts [8]. A straightforward application of their procedure to our present problem yields the dynamical evolution equations for the moving steps, starting from which many detailed analyses can be made.

Consider an infinite train of nonoverlapping steps on the crystal surface shown schematically in Fig. 1. The time-dependent position of the nth step is parametrized by $z=\zeta^n(x,t)$. In a coordinate frame moving with velocity V in the positive z direction, the free boundary problem takes the form

$$\left[\nabla^2+V\frac{\partial}{\partial z}-1-\frac{\partial}{\partial t}\right]u(x,z,t)=0 \ , \tag{3.1}$$

$$\left[V+\frac{d\zeta^n}{dt}\right]dx=-[(\nabla u)^n_+-(\nabla u)^n_-]\cdot d\sigma^n \ , \tag{3.2}$$

$$u(x,\zeta^n,t)=\Delta-d_0\kappa\{\zeta^n\} \ , \tag{3.3}$$

where the superscripts label the steps and the vector step length element $d\sigma$ is defined according to Fig. 1. To proceed, we define a Green's function in the moving frame by

$$\left[\nabla_1^2-V\frac{\partial}{\partial z_1}-1+\frac{\partial}{\partial t_1}\right]G(p|p_1)=-\delta(p-p_1) \ , \tag{3.4}$$

with the short notation $p=(x,z,t), p_1=(x_1,z_1,t_1)$. The causality condition that $G(p|p_1)=0$ for $t<t_1$ is also imposed. For an arbitrary space-time point p, we have, from (3.1) and (3.4),

$$\begin{aligned}u(p)=&\int_{-\infty}^{t}dt_1\int_{S_1}d\sigma_1\cdot[u(p_1)\nabla_1 G(p|p_1)\\&-G(p|p_1)\nabla_1 u(p_1)]\\&+V\int_{-\infty}^{t}dt_1\int_{\Lambda_1}dx_1dz_1\frac{\partial}{\partial z_1}[u(p_1)G(p|p_1)] \ ,\end{aligned} \tag{3.5}$$

where the Green's theorem has been applied to the region Λ_1 containing the point p but excluding all the steps bounded by the boundary surface S_1. The volume contribution in (3.5) vanishes identically because the integration over dz_1 gives canceling terms from two sides of each step. This cancellation is specific to the symmetric model, where the continuity of adatom density across each step is maintained. Further application of this continuity property to the first part of the surface integral in (3.5) also gives a null result. Hence (3.5) reduces to

$$u(p)=\sum_{m=-\infty}^{+\infty}\int_{-\infty}^{t}dt_1\int_{p_1\in m}G(p|p_1\{[\nabla_1 u(p_1)]_--[\nabla_1 u(p_1)]_+\}\cdot d\sigma_{1+} \ , \tag{3.6}$$

which, upon using the boundary condition (3.2) and letting p approach the nth step, leads to the equation of motion for the nth step:

$$\Delta-d_0\kappa\{\zeta^n\}=\sum_{m=-\infty}^{+\infty}\int_{-\infty}^{t}dt_1\int_{-\infty}^{+\infty}dx_1 G(x,\zeta^n,t|x_1,\zeta_1^m,t_1)\left[V+\frac{d\zeta_1^m}{dt_1}\right] . \tag{3.7}$$

Here the curvature is by definition

$$\kappa\{\zeta^n\}=-\frac{d^2\zeta^n}{dx^2}\left[1+\left[\frac{d\zeta^n}{dx}\right]^2\right]^{-3/2}. \tag{3.8}$$

This set of closed, nonlinear, integro-differential equations describes the time-dependent evolution of an infinite train of steps mutually coupled through the overlapping adatom diffusion fields. With little modification, the boundary integral approach can also be used to investigate pattern selection problems for spiral steps. Finally, we point out that, in the present consideration, no energetic interaction between steps, such as that due to elasticity, is yet incorporated.

IV. LINEAR STABILITY ANALYSIS

The boundary integral formulation makes possible certain analytical treatments otherwise infeasible using the original full diffusion model. For example, this approach is particularly suitable for determining various steady state solutions and for analyzing their stabilities. Although Eq. (3.7) supports in general steady state solutions of both straight and curved steps, we restrict our consideration in this paper to straight steps only.

This section presents a linear stability analysis of uniformly moving step trains. The advantages of using (3.7) for linear stability analysis, rather than using the full diffusion equation, are twofold. First the method is systematic and allows us to treat simultaneously perturbations both along and perpendicular to the steps. Second, the calculation can be carried out without having to use the quasistatic approximation, which becomes unreliable for both fast-moving and densely packed step trains. The situation of fast step trains is likely to occur in molecular beam epitaxy (MBE) growth where the dimensionless supersaturation is typically large [3]. Some of our results reported here were previously known but were obtained using different methods under quasistatic approximations.

First we concentrate on steady state solutions for straight steps. Consider an infinite train of equidistant steps moving uniformly with velocity V in the positive z direction. In the comoving frame of the steps, letting $\zeta^n(x,t)=n\lambda$ with λ being the step spacing, and using the real-space representation of the Green's function

$$G(p|p_1)=\frac{e^{-(t-t_1)}}{4\pi(t-t_1)}\exp\left[-\frac{(x-x_1)^2+[z-z_1+V(t-t_1)]^2}{4(t-t_1)}\right], \tag{4.1}$$

we obtain, from (3.7),

$$\Delta=V\sum_{m=-\infty}^{+\infty}\int_0^{+\infty}d\tau\int_{-\infty}^{+\infty}dx_1\,G(0,0,\tau|x_1,m\lambda,0), \tag{4.2}$$

which leads to the transcendental equation [3]

$$2\Delta=\left[\frac{\alpha_+-\alpha_-}{\alpha_++\alpha_-}\right]\left[\coth\frac{\alpha_+\lambda}{2}+\coth\frac{\alpha_-\lambda}{2}\right], \tag{4.3}$$

where we have defined for convenience

$$\alpha_\pm\equiv\left[1+\frac{1}{l^2}\right]^{1/2}\pm\frac{1}{l}. \tag{4.4}$$

Equation (4.3) can be solved numerically for the velocity of steps $V=V(\Delta,\lambda)$, which is monotonically increasing in both Δ and λ.

Next let us analyze the morphological stability of this system of equidistant steps. Consider small-amplitude perturbations to the steady state step profiles in the general form

$$\hat{\zeta}^n(x,t)=\zeta^n(x,t)-n\lambda \tag{4.5}$$

for all n. Equations governing the time evolution of perturbations are derived by expanding (3.7) in powers of the small quantity $\hat{\zeta}^n$. We shall use the Green's function in a Fourier representation

$$G(p|p_1)=\int\frac{d\omega dk}{(2\pi)^2}e^{ik(x-x_1)+i\omega(t-t_1)}\times\frac{e^{-(\zeta^n-\zeta_1^m)/l-|\zeta^n-\zeta_1^m|M}}{2M(k,\omega)}, \tag{4.6}$$

where

$$M(k,\omega)\equiv\left[k^2+1+\frac{1}{l^2}+i\omega\right]^{1/2}, \tag{4.7}$$

with a positive real part. The integrand in the Green's function can be readily expanded to first order in perturbation to read

$$e^{-(\zeta^n-\zeta_1^m)/l-|\zeta^n-\zeta_1^m|M}=I_{nm}^{(0)}+I_{nm}^{(1)}+\cdots, \tag{4.8}$$

where the zeroth order term is given by

$$I_{nm}^{(0)}=e^{-(n-m)\lambda/l-|n-m|\lambda M} \tag{4.9}$$

and the first order term takes the form

$$I_{nm}^{(1)}=\begin{cases}-(\hat{\zeta}^n-\hat{\zeta}_1^n)/l-|\hat{\zeta}^n-\hat{\zeta}_1^n|M & \text{for } n=m\\ -(Ml+1)e^{-(M+1/l)(n-m)\lambda}(\hat{\zeta}^n-\hat{\zeta}_1^m)/l & \text{for } n>m\\ (Ml-1)e^{(M-1/l)(n-m)\lambda}(\hat{\zeta}^n-\hat{\zeta}_1^m)/l & \text{for } n<m.\end{cases} \tag{4.10}$$

Now these expressions can be inserted into the right-hand side of (3.7) which has the expansion

$$\int dt_1 dx_1 \frac{d\omega dk}{(2\pi)^2} \frac{e^{ik(x-x_1)+i\omega(t-t_1)}}{2M} \sum_m \left[\frac{d\hat{\zeta}_1^m}{dt_1} I_{nm}^{(0)} + V I_{nm}^{(1)} \right] . \tag{4.11}$$

It is more convenient to work in the Fourier space by defining Fourier transforms as, for example,

$$\hat{\zeta}^n(k,\omega) = \int_{-\infty}^{+\infty} dt \int dx \, e^{-ikx-i\omega t} \hat{\zeta}^n(x,t) . \tag{4.12}$$

After grouping together all the terms that are linear in perturbation in the expansion of Eq. (3.7), we obtain the linear stability equation

$$\mathcal{L}(k,\omega,\hat{\zeta}) = 0 , \tag{4.13}$$

where

$$\mathcal{L}(k,\omega,\hat{\zeta}) = \left[\frac{i\omega l^2}{2} + 1 - Ml \left[\Delta - d_0 l k^2 + \frac{1}{e^{\alpha_+ \lambda} - 1} - \frac{1}{e^{\alpha_- \lambda} - 1} \right] \right] \hat{\zeta}^n(k,\omega) + \left[\frac{i\omega l^2}{2} + 1 + Ml \right] \sum_{m<n} e^{-(M+1/l)(n-m)\lambda} \hat{\zeta}^m(k,\omega) + \left[\frac{i\omega l^2}{2} + 1 - Ml \right] \sum_{m>n} e^{-(M-1/l)(m-n)\lambda} \hat{\zeta}^m(k,\omega) . \tag{4.14}$$

Linear dispersion relations under general perturbations are solutions of (4.13), as we shall show below.

Before moving on, we reiterate that, although we have so far considered only straight steps, Eq. (3.7) also has steady state solutions corresponding to curved steps. In general, these solutions can be approximately evaluated, in the small-amplitude limit, by expanding (3.7) to higher orders in $\hat{\zeta}$. The linear stability of these solutions can in turn be similarly investigated. However, these calculations are in practice quite cumbersome [8].

A. Stability of an isolated step

As a special case, let us consider the linear stability of an isolated step. This situation is equivalent to the limit of infinite step spacing $\lambda = \infty$. Stability equation (4.13) simplifies to

$$\frac{i\omega l^2}{2} + 1 - (\Delta - d_0 l k^2) l M(k,\omega) = 0 , \tag{4.15}$$

which gives the linear dispersion relation in the closed form

$$\frac{i\omega l^2}{2} = (\Delta - d_0 l k^2) \sqrt{l^2 k^2 + l^2 - 1 + (\Delta - d_0 l k^2)^2} - 1 + (\Delta - d_0 l k^2)^2 , \tag{4.16}$$

where the quantity $l = \sqrt{1-\Delta^2}/\Delta$ is solved from (4.3). This dispersion relation is plotted in Fig. 2.

It is evident from Fig. 2 that, within a certain parameter range, a straight step becomes linearly unstable against infinitesimal, long-wavelength fluctuations. This diffusive instability is of the same nature as that discovered by Mullins and Sekerka [9] for planar solidification fronts. The relevance of Mullins-Sekerka instability in step flow was first pointed out by Bales and Zangwill [2]. The step problem in question here, although resembling closely that of solidification, has important differences, in two respects. First, in solidification, steady state planar fronts growing into supercooled liquid do not exist at general supercoolings, in contrast with the situation here where uniformly moving straight steps are valid solutions at arbitrary supersaturation. Second, a planar front in solidification is always linearly unstable to perturbations of sufficiently long wavelength, with the effect of surface tension merely stabilizing the front on short length scales. But, again by contrast, straight steps can be completely stabilized by strong enough line tension on all scales (see below). Both differences between the two problems are due to the presence of the extra length scale, the adatom diffusion length x_s, in the step problem.

It follows from (4.16) that, as long as $d_0 \geq l\Delta^3/2$, a straight step is linearly stable against all infinitesimal perturbations, i.e., $\mathrm{Re}(i\omega) \leq 0$ for all k. Since $l = \sqrt{1-\Delta^2}/\Delta$, this condition is equivalent to

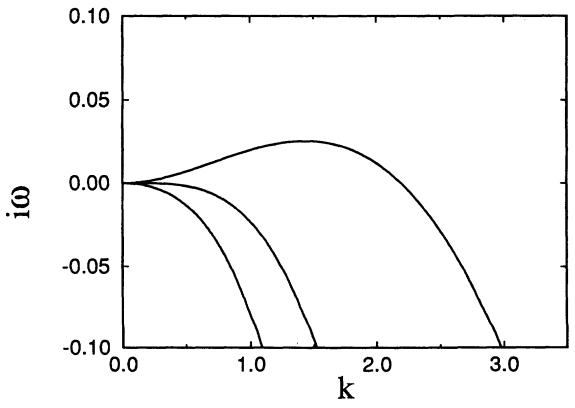

FIG. 2. Linear stability spectrum (4.16) of an isolated step against shape perturbations, in the symmetric model. Curves correspond, from top down, to values of line tension (d_0) 0.25, 1, and 2 times the critical value $\Delta^2\sqrt{1-\Delta^2}/2$.

$$d_0 \geq \frac{\Delta^2\sqrt{1-\Delta^2}}{2} . \tag{4.17}$$

On the other hand, for smaller values of d_0, the straight step is unstable against long-wavelength perturbations. The critical wave number below which perturbation grows is given bv

$$k_c = \left[\frac{\Delta}{d_0 l}\right]^{1/2}\left[1-\frac{d_0}{2\Delta^3 l}-\left[\frac{d_0}{\Delta^3 l}+\frac{d_0^2}{4\Delta^6 l^2}\right]^{1/2}\right]^{1/2} . \tag{4.18}$$

To see if (4.17) can be satisfied in realistic experimental situations, we estimate various quantities using values typical to crystal growth from solution. As an example, usual crystal growth from solution has a value of supersaturation $(c_\infty - c_0)/c_0 \approx 10^{-2}$. Further, we use $\gamma\Omega/k_B T = 25$ Å, $c_{eq}/c_r = 10^{-2}$, $x_s = 800$ Å, for NaCl crystals at $T = 600$ K. This gives an estimate that $d_0 \approx 3\times 10^{-4}$, $\Delta \approx 10^{-4}$, and therefore $d_0/\Delta^2 \gg 1$. Thus (4.17) is most likely to hold for conventional crystal growth, implying complete linear stability of straight steps. However, instability may occur under MBE growth situations where much higher supersaturation can be achieved, as suggested in Ref. [3]. Of course, at higher supersaturation, the nucleation of adatom islands on the otherwise flat terraces becomes important and can no longer be neglected. Eventually, for sufficiently large supersaturation, we expect the layer-by-layer growth picture underlying the BCF model to break down completely, and the growth of crystal should proceed three dimensionally.

Although (4.17) is derived within the symmetric model, the qualitative conclusion, that there exists a critical value of line tension above which the step is linearly stable, is unaltered when asymmetric attachment kinetics are taken into account. Only the numerical value of the threshold (4.17) is modified. It will be shown later that in a one-sided model with strong attachment kinetics, the threshold (4.17) changes to $d_0 \geq \Delta/2$. So step instability is relatively easier to realize, even for the parameters of conventional crystal growth quoted above.

B. Stability of step train under lateral fluctuations

We now examine the linear stability of an infinite train of equidistant steps. It is useful to distinguish two types of morphological perturbations: the lateral fluctuations to the shapes of steps, and the longitudinal displacement of steps from steady state positions. Both kinds of perturbations are accounted for simultaneously in the stability equation (4.13).

In this section we first investigate the linear stability of steps with respect to fluctuations of the first type, assuming to this end that the average spacing between steps is maintained at fixed value λ. Still, shape perturbations on different steps need not be synchronous, but the most unstable situation corresponds to all steps having in-phase fluctuations. That is, $\hat{\zeta}^m(k,\omega) = \hat{\zeta}^n(k,\omega)$ for arbitrary m,n. In this case, Eq. (4.13) yields

$$\frac{1}{lM}\left[\frac{i\omega l^2}{2}+1\right]\left[\coth\left[M+\frac{1}{l}\right]\frac{\lambda}{2}+\coth\left[M-\frac{1}{l}\right]\frac{\lambda}{2}\right] + \left[\coth\left[M+\frac{1}{l}\right]\frac{\lambda}{2}-\coth\left[M-\frac{1}{l}\right]\frac{\lambda}{2}\right] = 2(\Delta - d_0 l k^2)+\left[\coth\frac{\alpha_+\lambda}{2}-\coth\frac{\alpha_-\lambda}{2}\right], \tag{4.19}$$

which can be solved implicitly for the dispersion relation $\omega = \omega(k)$. The presence of a zero mode in the spectrum, due to the translational invariance of the steady state solution, is evident by explicit inspection: $\omega = k = 0$ solves (4.19). Unfortunately, Eq. (4.19) does not afford an explicit analytic solution of $\omega(k)$. However, one can still demonstrate that steps become completely linearly stable for strong enough line tension. The critical value of the dimensionless capillary length is determined via the condition

$$\left.\frac{d^2\omega(k)}{dk^2}\right|_{k=0} = 0 ,$$

which gives the formula for the threshold line tension:

$$d_0 \geq \frac{\alpha_+ - \alpha_-}{(\alpha_+ + \alpha_-)^2}\left[\Delta + \frac{\alpha_+\lambda e^{\alpha_+\lambda}}{(e^{\alpha_+\lambda}-1)^2} - \frac{\alpha_-\lambda e^{\alpha_-\lambda}}{(e^{\alpha_-\lambda}-1)^2}\right] , \tag{4.20}$$

where $\alpha_\pm = \alpha_\pm(\Delta,\lambda)$ have been defined previously and can be solved from the steady state solution (4.3). Two limits, of large and small step spacing, respectively, are analytically tractable. Specifically, we obtain from (4.3) that

$$\alpha_+ = 1 + \frac{\Delta}{2}\lambda + \cdots \tag{4.21}$$

for $\lambda \ll 1$ and

$$\alpha_+ = \left[\frac{1+\Delta}{1-\Delta}\right]^{1/2}\left[1+\frac{\Delta}{1-\Delta^2}\left[e^{-\sqrt{[(1-\Delta)/(1+\Delta)]}\lambda}+e^{-\sqrt{[(1+\Delta)/(1-\Delta)]}\lambda}\right]+\cdots\right] \tag{4.22}$$

for $\lambda \gg 1$. Then condition (4.20) reduces, in the two limits, to

$$d_0 \geq \frac{\Delta^2}{360}\lambda^5 + O(\lambda^7) \tag{4.23}$$

for $\lambda \ll 1$ and

$$d_0 \geq \frac{\Delta^2\sqrt{1-\Delta^2}}{2} - \frac{\Delta\lambda}{2}\left[(1-\Delta)e^{-\sqrt{[(1-\Delta)/(1+\Delta)]}\lambda} - (1+\Delta)e^{-\sqrt{[(1+\Delta)/(1-\Delta)]}\lambda}\right] + \cdots \quad (4.24)$$

for $\lambda \gg 1$. Hence the critical value of d_0 needed to linearly stabilize straight steps of finite spacing against lateral perturbations is always smaller than that required for an isolated step. This observation is consistent with the intuitive expectation that smaller λ suppresses lateral fluctuations of the steps, due to greater overlap of adatom diffusion fields. For asymmetric attachment kinetics, this conclusion remains qualitatively true as well, and has been reached by previous authors [2] using quasistatic analyses.

Our analysis is strictly linear and therefore does not address the inquiry regarding what happens once straight steps become linearly unstable. A natural expectation is that the steps may adopt profiles corresponding to other steady state solutions. A recent nonlinear, quasistationary analysis by Misbah and Rappel [10] for the asymmetric model established the existence of cellular step solutions with a continuum band of possible wavelengths. Whether or which of these solutions can be actually selected is intimately related to their stability, an issue which remains unresolved.

C. Stability of step train under longitudinal fluctuations

We now investigate the linear stability of an infinite step train against perturbations in the distances between steps. In this situation, an instability could lead to the coalescence or bunching of individual monoatomic steps into multiple-step bands, a feature frequently observed during crystal morphological changes. For simplicity, we assume that the line tension is large enough so that all steps remain flat so that we can set $k=0$ in the stability equation. Arbitrary displacement of steps from their steady state positions can be decomposed into the normal modes as $\hat{\zeta}^n(k,\omega)=e^{iq\lambda n}u_q$, with q being the real wave number. Without loss of generality, the wave number q can be further restricted to its first Brillouin zone $q\in[-\pi/\lambda,\pi/\lambda]$. The stability equation (4.13) then reads

$$\sum_{n=-\infty}^{+\infty} A_n(i\omega)e^{iq\lambda n}=0 , \quad (4.25)$$

where the coefficients $A_n(i\omega)$ are given by

$$A_0(i\omega)=\frac{i\omega l^2}{2}+1-\hat{M}\left[\Delta+\frac{1}{e^{\alpha_+\lambda}-1}-\frac{1}{e^{\alpha_-\lambda}-1}\right] , \quad (4.26)$$

$$A_{n>0}(i\omega)=\left[\frac{i\omega l^2}{2}+1-\hat{M}\right]e^{-(\hat{M}-1)n\lambda/l} , \quad (4.27)$$

$$A_{n<0}(i\omega)=\left[\frac{i\omega l^2}{2}+1+\hat{M}\right]e^{(\hat{M}+1)n\lambda/l} , \quad (4.28)$$

where $\hat{M}(i\omega)\equiv lM(k=0,\omega)=\sqrt{l^2+1+i\omega l^2}$. The frequency ω is in general complex, so it is appropriate to separate the dispersion relation into a real and an imaginary part, $i\omega(q)=\Omega_R(q)+i\Omega_I(q)$. Positive values of Ω_R imply exponential amplification of small perturbations hence linear instability. Once again one can check by explicit substitution the presence of a translational zero mode $\Omega_R(q=0)=\Omega_I(q=0)=0$.

First let us examine in detail the analytically tractable limit of long-wavelength perturbations $|q\lambda| \ll 1$, corresponding to dispersion spectrum near the center of the Brillouin zone. Taylor expansion of the stability equation gives in this limit the relations

$$\Omega_I(q)=-\frac{\sum nA_n}{\sum A_n'}(q\lambda)+O((q\lambda)^3) , \quad (4.29)$$

$$\Omega_R(q)=\frac{\sum A_n''}{2\sum A_n'}\Omega_I^2+\frac{\sum nA_n'}{\sum A_n'}(q\lambda)\Omega_I + \frac{\sum n^2A_n}{2\sum A_n'}(q\lambda)^2+O((q\lambda)^4) , \quad (4.30)$$

where primes denote derivatives with respect to $i\omega$ evaluated at $i\omega=0$. Note that in the long-wavelength limit, $\Omega_I(q)$ is linear but $\Omega_R(q)$ is quadratic in the wave number. Formula (4.29) can be evaluated to give

$$\Omega_I(q)=\frac{(\alpha_++\alpha_-)\left[\alpha_+\sinh^{-2}\frac{\alpha_+\lambda}{2}+\alpha_-\sinh^{-2}\frac{\alpha_-\lambda}{2}\right]}{4\Delta l^2-\lambda\alpha_+\sinh^{-2}\frac{\alpha_+\lambda}{2}+\lambda\alpha_-\sinh^{-2}\frac{\alpha_-\lambda}{2}}q\lambda . \quad (4.31)$$

The expression for the real mode is much more complicated and is not displayed here. Despite the complexity, behavior in the limits of large and small step spacings can still be extracted, using the expansions (4.21) and (4.22). The results are, for $\lambda \gg 1$,

$$\Omega_I(q)=\frac{2\Delta}{(1-\Delta^2)(1+\Delta)} \times\left[e^{-\sqrt{[(1-\Delta)/(1+\Delta)]}\lambda} +\frac{1+\Delta}{1-\Delta}e^{-\sqrt{[(1+\Delta)/(1-\Delta)]}\lambda}+\cdots\right]q\lambda\ , \tag{4.32}$$

$$\Omega_R(q)=\frac{-\Delta^2}{(1-\Delta^2)(1+\Delta)} \times\left[e^{-\sqrt{[(1-\Delta)/(1+\Delta)]}\lambda} -\frac{1+\Delta}{1-\Delta}e^{-\sqrt{[(1+\Delta)/(1-\Delta)]}\lambda}+\cdots\right](q\lambda)^2\ , \tag{4.33}$$

and for $\lambda \ll 1$,

$$\Omega_I(q)=[\Delta+O(\lambda^2)]q\lambda\ , \tag{4.34}$$

$$\Omega_R(q)=\left[-\frac{\Delta^2(1+3\Delta^2)}{12}\lambda^2+O(\lambda^4)\right](q\lambda)^2\ . \tag{4.35}$$

These asymptotic expansions are obtained from the full linear stability equation, hence involve no approximations. We note in particular that our result for $\Omega_I(q)$ agrees with that of Bennema and Gilmer [11], obtained in a simple model assuming a step velocity depending upon only nearest terrace widths. Most importantly, however, in contrary to a pure neutral mode $\Omega_R(q)=0$ found in their approximate model, we obtain a weakly stable mode $\Omega_R \le 0$.

While the magnitude of $\Omega_R(q)$ reflects the typical decay or amplification rate of perturbations, $\Omega_I(q)$ is related to the wave velocity for the propagation of disturbances. When the wavelength of disturbances is large compared with the step spacing, i.e., $q\lambda \ll 1$, the group velocity of disturbances coincides with the phase velocity since $\Omega_I(q)$ is linear in q. Both are given by $v=-\Omega_I/q$ in the comoving frame. We immediately see that for small step spacing $\lambda \ll 1$, $v=-V$, so the disturbances remain stationary in the laboratory frame. On the other hand, for large step separation $\lambda \gg 1$, $v=0$, and the disturbances propagate along with the steps.

The exact linear stability spectrum (4.25) over the complete Brillouin zone can only be solved numerically. However, we can attempt an approximate solution utilizing a quasistatic approximation. As is usually done, this approximation assumes that the diffusion field adjusts quickly in response to the displacement of the steps. It amounts to neglecting the frequency dependence, or the memory effect, in the Green's function: $\hat{M}(i\omega)=\sqrt{l^2+1}+i\omega l^2 \approx \sqrt{l^2+1}$. Now (4.25) can be easily solved over the whole Brillouin zone to yield

$$\Omega_R(q)=\frac{2}{l^2}\left\{\left[\Delta+\frac{1}{e^{\alpha_+\lambda}-1}-\frac{1}{e^{\alpha_-\lambda}-1}\right]\sqrt{1+l^2} \times\coth\left[\lambda\left[1+\frac{1}{l^2}\right]^{1/2}\right]-1\right\}(1-\cos q\lambda)\ , \tag{4.36}$$

$$\Omega_I(q)=\frac{2\sqrt{1+l^2}\sinh(\lambda/l)}{l^2\sinh(\lambda\sqrt{1+1/l^2})} \times\left[\coth\frac{\lambda}{l}-\Delta-\frac{1}{e^{\alpha_+\lambda}-1}+\frac{1}{e^{\alpha_-\lambda}-1}\right]\sin q\lambda\ . \tag{4.37}$$

The quasistatic dispersion relation is shown, in dashed lines, along with the numerically determined exact spectrum, in Fig. 3. The most important feature is that $\Omega_R(q)\le 0$ for all q, suggesting complete linear stability of the equidistant step train against fluctuations in step spacings.

To suppress the frequency dependence in $\hat{M}(i\omega)$ when adopting the quasistatic approximation, we need $|\omega| \ll 1$. From the quasistatic spectrum, it can be seen that typically $\Omega_I=O(\Delta)$ and $\Omega_R=O(\Delta^2)$. Hence the condition of small supersaturation $\Delta \ll 1$ is necessary. Another, more subtle, source of inaccuracy may occur in the quasistatic procedure, if the magnitudes of Ω_R and Ω_I have large disparity between them. This seems to explain the discrepancies between the quasistatic and the exact spec-

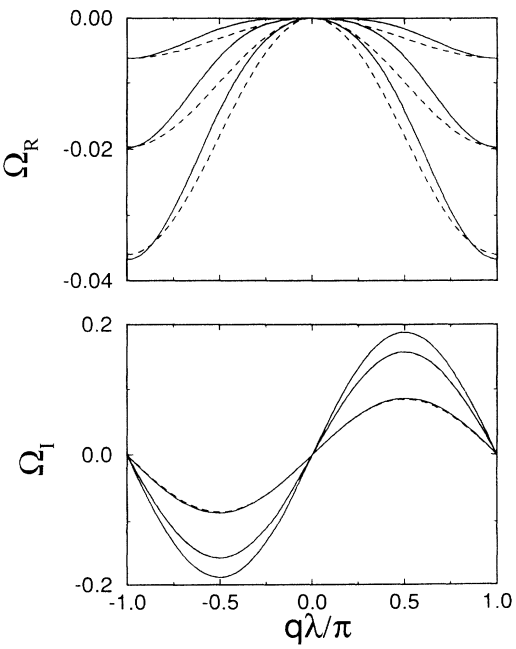

FIG. 3. Dispersion relation of an infinite train of parallel steps against perturbations in step spacings, in the symmetric model. Solid lines are obtained numerically from (4.25), and dashed lines correspond to the quasistatic spectrum (4.36) and (4.37). Curves in the upper figure, from top down, are for $\lambda=0.5$, 1, and 2. Order of curves is reversed in the lower part.

tra near the center of the Brillouin zone for small λ in Fig. 3.

V. GROWTH AND EVAPORATION WITH ASYMMETRIC ATTACHMENT KINETICS

In the preceding discussions, steps are assumed to be ideal line sources or sinks near which a continuous adatom density is maintained at the local equilibrium value. This picture must be modified, in several respects, to accommodate to more realistic growth situations. First of all, effects such as the finite rate of adatom exchange at steps, insufficient concentration, and nonideal distribution of sink sites on steps, all lead to deviations of adatom density at the steps from the equilibrium value. In other words, growth rate is no longer solely controlled by adatom transport, but also by interface kinetics. Secondly, atomic exchanges on different sides of steps involve different kinetic barriers and are therefore nonequivalent. This asymmetry in attachment kinetics was pointed out by Schwoebel and Shipsey [6], and discussed extensively in subsequent literature. Lastly, interface kinetics usually exhibit pronounced anisotropy.

The effect of interface kinetics is usually taken into account by assuming an elevation of c_{step} from the equilibrium value linearly proportional to the adatom flux. Accordingly boundary condition (2.3) is replaced by

$$c_{\text{step}\pm}-c_0\left[1+\frac{\gamma\Omega}{k_BT}\kappa\right]=\beta_{\pm}D(\nabla c)\cdot\mathbf{n}_{\pm}\ , \tag{5.1}$$

where differences in the coefficients $\beta_{\pm}$ measure the asymmetry of attachment kinetics. We have for simplicity neglected the effect of anisotropy. In this section, we consider a situation with the most asymmetry, assuming local equilibrium near lower terraces but complete inhibition of adatom exchange from upper terraces. This amounts to setting $\beta_+=0$, $\beta_-=\infty$ in (5.1). We further distinguish between two particular cases of crystal growth and evaporation, respectively, shown schematically in Fig. 4. Again working in the moving frame with velocity V in the z direction, the boundary conditions (3.2) and (3.3) are modified to the dimensionless form

$$\left[V+\frac{d\zeta^n}{dt}\right]dx=-(\nabla u)^n_+\cdot d\sigma^n,\quad (\nabla u)_-\cdot d\sigma^n=0\ , \tag{5.2}$$

$$u_+(x,\zeta^n,t)=\Delta-d_0\kappa\{\zeta^n\} \tag{5.3}$$

for the case of growth and

$$\left[V+\frac{d\zeta^n}{dt}\right]dx=(\nabla u)^n_-\cdot d\sigma^n,\quad (\nabla u)_+\cdot d\sigma^n=0\ , \tag{5.4}$$

$$u_-(x,\zeta^n,t)=\Delta-d_0\kappa\{\zeta^n\} \tag{5.5}$$

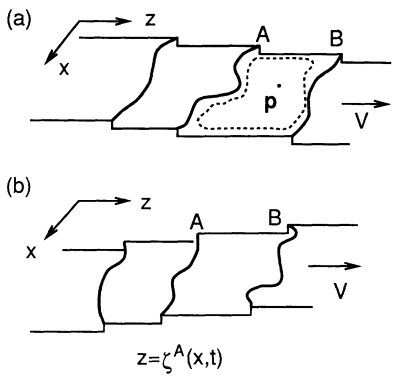

FIG. 4. Schematic representation of step flow during (a) crystal growth and (b) evaporation with asymmetric attachment kinetics.

for the case of evaporation. The bulk diffusion equation (3.1) remains intact in both cases. Note, however, that for evaporation, the quantity Δ (>0) is identified with the dimensionless undersaturation and the dimensionless diffusion field in this case is defined according to $u=(c-c_\infty)/c_r$ in contrast with (2.4). The above models are analogies of the one-sided models in solidification.

A. The case of growth

Integro-differential equations for the step displacement are derived using the same method as before by applying Green's theorem to the domain shown in Fig. 4. Since adatom density will not be continuous across a step, twice as many equations are needed compared to the symmetric case. A static version of the Green's function method was recently used by Misbah and Rappel [10] in a bifurcation study of the steady state solution of cellular steps.

Consider an arbitrary point $p\in\Lambda_1$ on the terrace between steps A and B in Fig. 4. Green's theorem gives

$$\begin{aligned}u(p)=&\int_A dx_1 G(p|p_1)\left[V[1-u^A_+(p_1)]+\frac{d\zeta_1^A}{dt_1}\right]\\&+\int_A d\sigma_1 u^A_+(p_1)\cdot\nabla_1 G(p|p_1)\\&+\int_B d\sigma_1 u^B_-(p_1)\cdot\nabla_1 G(p|p_1)\\&+V\int_B dx_1 u^B_-(p_1)G(p|p_1)\ ,\end{aligned} \tag{5.6}$$

where to save notation the integration over dt_1 is implied in the above expression. When we let the point p approach step A, the second term on the right-hand side with $\nabla_1 G$ develops an integrable singularity. After separating the contribution of this singularity, we obtain

$$\begin{aligned}u^A_+(\zeta^A,t)=&2\int_B d\sigma_1 u^B_-(p_1)\cdot\nabla_1 G(p|p_1)+2V\int_B dx_1 u^B_-(p_1)G(p|p_1)\\&+\int_A dx_1\left[V[2-u^A_+(p_1)]+2\frac{d\zeta_1^A}{dt_1}+\left[\zeta^A-\zeta_1^A-\frac{d\zeta_1^A}{dx_1}(x-x_1)\right]\frac{u^A_+(p_1)}{t-t_1}\right]G(p|p_1)\ .\end{aligned} \tag{5.7}$$

Another equation is similarly obtained letting p approach step B,

$$u_-^B(\xi^B,t)=2\int_A d\sigma_1 u_+^A(p_1)\cdot\nabla_1 G(p|p_1)+2\int_A dx_1\left[V(1-u_+^A)+\frac{d\xi_1^A}{dt_1}\right]G(p|p_1)$$
$$+\int_B dx_1 G(p|p_1)\left[V-\left[\xi^B-\xi_1^B-\frac{d\xi_1^B}{dx_1}(x-x_1)\right]\frac{u_-^B(p_1)}{t-t_1}\right]. \tag{5.8}$$

Once again, linearization of (5.7) and (5.8) leads to the stability equation. Here we first briefly mention the linear stability of an isolated straight step under lateral shape perturbations. In our formalism, it turns out the dispersion relation can again be solved closely, from the relation

$$i\omega l^2+2=(\Delta-d_0 lk^2)(lM+1)$$
$$+\Delta l(k^2 l+\sqrt{1+l^2}M-lM^2), \tag{5.9}$$

where $M(k,\omega)=\sqrt{k^2+1+1/l^2+i\omega}$. The actual expression for $\omega(k)$ is lengthy and not shown here. We only point out that the threshold line tension needed to linearly stabilize the straight step is now given by

$$d_0\geq\frac{\Delta\sqrt{1-\Delta}}{2-\Delta}, \tag{5.10}$$

while for smaller d_0 the step is unstable to long-wavelength perturbations. Thus suppressing adatom attachment from the upper terrace makes the step more susceptible to shape fluctuations. Further, it can be shown that the effect of finite step spacing λ is stabilizing, which merely reduces the above threshold to smaller values. The calculation is straightforward and reproduces the results of previous authors [2].

Below, our major attention will be paid to the longitudinal modes of an infinite step train. For straight steps, the equations of motion are much simpler. Since $u_+^A=\Delta$ and $\zeta(x,t)$ is independent of x, the integration over dx_1 can be carried out explicitly. And the equations for steps A and B are

$$\Delta=\int dt_1\left[V(2-\Delta)+2\frac{d\xi_1^A}{dt_1}\right]G(\xi^A,t|\xi_1^A,t_1)$$
$$+2\int dt_1 u_-^B(t_1)$$
$$\times[VG(\xi^A,t|\xi_1^B,t_1)-\nabla_{1z}G(\xi^A,t|\xi_1^B,t_1)], \tag{5.11}$$

$$u_-^B(t)=\int dt_1\left[2V(1-\Delta)+2\frac{d\xi_1^A}{dt_1}\right]G(\xi^B,t|\xi_1^A,t_1)$$
$$+2\Delta\int dt_1\nabla_{1z}G(\xi^B,t|\xi_1^A,t_1)$$
$$+V\int dt_1 u_-^B(t_1)G(\xi^B,t|\xi_1^B,t_1), \tag{5.12}$$

with the reduced Green's function

$$G(zt|z_1t_1)=\frac{e^{-(t-t_1)}}{\sqrt{4\pi(t-t_1)}}$$
$$\times\exp\left[-\frac{[z-z_1+V(t-t_1)]^2}{4(t-t_1)}\right]. \tag{5.13}$$

Uniformly moving steady states are zeroth order solutions of (5.11) and (5.12). Setting $\zeta^A=0,\zeta^B=\lambda$, we obtain

$$u_-=e^{-\alpha_+\lambda}(\alpha_+^2+\Delta-1)=e^{\alpha_-\lambda}(\alpha_-^2+\Delta-1), \tag{5.14}$$

from which both the velocity of the step and the adatom density at the upper side of the steps can be calculated. And the magnitude of discontinuity in adatom density across the step equals $\Delta-u_-$.

The linear stability equation, derived from (5.11) and (5.12) by linearization, follows the same structure as (4.25), but with only two terms $n=0,1$ in the summation. It reads

$$\frac{\hat{M}-1}{\hat{M}+1}e^{(\hat{M}-1)\lambda/l}[i\omega l^2+2-\Delta-2\hat{M}+\Delta\hat{M}\sqrt{1+l^2}]$$
$$+e^{-(\hat{M}+1)\lambda/l}[i\omega l^2+2-\Delta+2\hat{M}+\Delta\hat{M}^2]$$
$$=u_-e^{iq\lambda}\hat{M}(\hat{M}+\alpha_- l-1), \tag{5.15}$$

where as before $\hat{M}(i\omega)=\sqrt{1+l^2+i\omega l^2}$. It is easier in this case to extract the dispersion relation near the center of the Brillouin zone. We find, to leading order, that

$$\Omega_I(q)=\frac{2\Delta(2-\Delta)^3}{(1-\Delta)^2(4-2\Delta-\Delta^2)}e^{-[(2-\Delta)/\sqrt{1-\Delta}]\lambda}q\lambda, \tag{5.16}$$

$$\Omega_R(q)=\frac{-\Delta(2-\Delta)^3}{(1-\Delta)^2(4-2\Delta-\Delta^2)}e^{-[(2-\Delta)/\sqrt{1-\Delta}]\lambda}(q\lambda)^2 \tag{5.17}$$

in the limit of large step separation $\lambda\gg1$ and

$$\Omega_I(q)=[\Delta+O(\lambda^2)]q\lambda, \tag{5.18}$$

$$\Omega_R(q)=-\left[\frac{\Delta}{2}+\Delta^2+\frac{3\Delta^3}{32}+O(\lambda^2)\right](q\lambda)^2 \tag{5.19}$$

in the limit of narrow step trains. The spectrum solved under the quasistatic approximation also takes a particularly simple form:

$$\Omega_I(q)=\frac{u_-^2e^{2\lambda/l}}{\Delta}\sin q\lambda, \tag{5.20}$$

$$\Omega_R(q)=-\frac{u_-^2e^{2\lambda/l}}{\Delta}(1-\cos q\lambda). \tag{5.21}$$

Note that both Ω_R and Ω_I are of the same order $O(\Delta)$. In Fig. 5, a comparison of the exact spectrum with the quasistatic one suggests the latter to be a very good approximation. Since $\Omega_R(q)\leq0$ for all q, the infinite step strain is linearly stable against perturbations in step spacings.

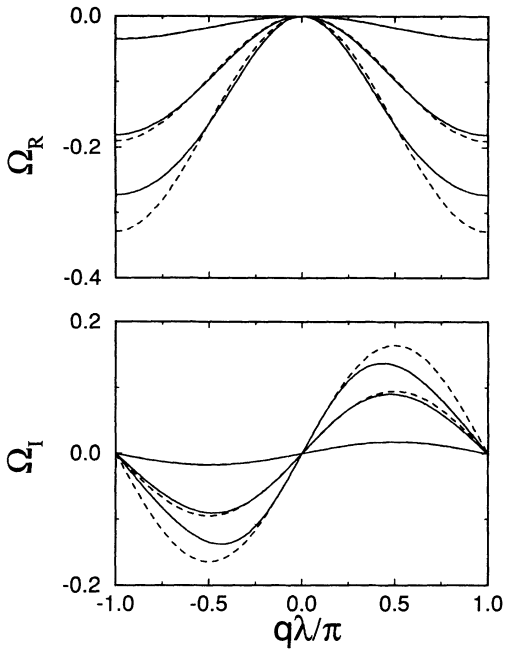

FIG. 5. Dispersion relation of an infinite train of parallel steps against perturbations in step spacings during crystal growth, in the one-sided model. Solid lines represent the numerically solved exact spectrum, and dashed lines correspond to the quasistatic spectrum. Curves, in increasing amplitude, are for $\lambda=2$, 1, and 0.5.

B. The case of evaporation

With little modification, procedures used in the last subsection can be applied to the case of crystal evaporation. We will not repeat the analyses, but only quote the results. For an isolated straight step, the linear stability spectrum for lateral fluctuations is the closed solution of

$$i\omega l^2+2=(\Delta-d_0 lk^2)(lM-1) -\Delta l(k^2 l+\sqrt{1+l^2}M-lM^2) . \quad (5.22)$$

It follows that $i\omega$ is pure real and $i\omega(k)\leq 0$, for arbitrary d_0 and k. So a straight step is completely linear stable against shape fluctuations. This conclusion remains valid for equidistant step trains with finite λ as well.

The equations of motion for parallel steps resemble those in the case of growth and read

$$\Delta=\int dt_1\left[V(2+\Delta)+2\frac{d\zeta_1^B}{dt_1}\right]G(\zeta^B,t|\zeta_1^B,t_1) -2\int dt_1 u_+^A(t_1) \times[VG(\zeta^B,t|\zeta_1^A,t_1)-\nabla_{1z}G(\zeta^B,t|\zeta_1^A,t_1)] , \quad (5.23)$$

$$u_+^A(t)=\int dt_1\left[2V(1+\Delta)+2\frac{d\zeta_1^B}{dt_1}\right]G(\zeta^A,t|\zeta_1^B,t_1) -2\Delta\int dt_1\nabla_{1z}G(\zeta^A,t|\zeta_1^B,t_1) -V\int dt_1 u_+^A(t_1)G(\zeta^A,t|\zeta_1^A,t_1) . \quad (5.24)$$

Stationary state adatom density and step velocity can be solved from

$$u_+=e^{-\alpha_-\lambda}(1+\Delta-\alpha_-^2)=e^{\alpha_+\lambda}(1+\Delta-\alpha_+^2) \quad (5.25)$$

and the linear stability equation is

$$\frac{\hat{M}+1}{\hat{M}-1}e^{(\hat{M}+1)\lambda/l}[i\omega l^2+2+\Delta+2\hat{M}-\Delta\hat{M}\sqrt{1+l^2}] +e^{-(\hat{M}-1)\lambda/l}[i\omega l^2+2+\Delta-2\hat{M}-\Delta\hat{M}^2] =-u_+e^{-iq\lambda}\hat{M}(\hat{M}+\alpha_+ l+1) . \quad (5.26)$$

The quasistatic dispersion relation,

$$\Omega_I(q)=\frac{u_+^2e^{-2\lambda/l}}{\Delta}\sin q\lambda , \quad (5.27)$$

$$\Omega_R(q)=\frac{u_+^2e^{-2\lambda/l}}{\Delta}(1-\cos q\lambda) , \quad (5.28)$$

is displayed in Fig. 6 with the exact spectrum. We immediately observe that $\Omega_R(q)\geq 0$ for all values of q. Therefore, while the infinite step train is linearly stable against lateral shape fluctuations, it is unstable to perturbations in step spacings, of all wavelengths.

VI. MORPHOLOGICAL FLUCTUATIONS OF STEPS

At finite temperatures, a monoatomic step on a singular crystal surface contains kink excitations. As the temperature is raised, the density of kink and other short-range structural excitations increases and the step can be-

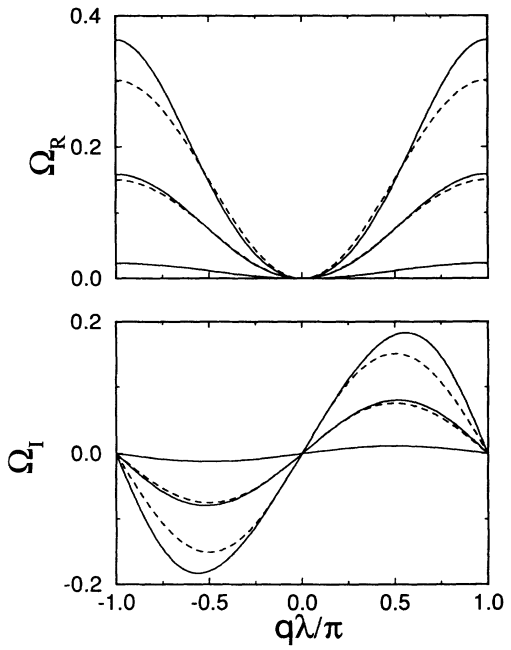

FIG. 6. Dispersion relation of an infinite train of parallel steps against perturbations in step spacings during evaporation, in the one-sided model. Numerically solved exact spectrum is shown in solid lines, and the quasistatic spectrum is shown in dashed lines. Curves, in increasing amplitude, correspond to $\lambda=2$, 1, and 0.5.

come molecularly rough. In fact, in our previous considerations of step kinetics, molecular roughness of steps is necessary for them to behave as good sources and/or sinks of adatoms so that the continuum description applies. Moreover, roughness of steps can persist to macroscopic scales comparable to step extension, since a step is always thermodynamically rough at finite temperature meaning that the amplitude of fluctuations diverges with the system size. Besides contribution from equilibrium fluctuations, step roughness is also affected by nonequilibrium properties of the growth process itself, for example, by the amplification of noises by the Mullins-Sekerka instability as we shall show below.

Previous studies of step morphology were mostly confined to treatments of the equilibrium fluctuations on weakly interacting steps [12]. In addition, the effect of thermal and other excitations on the terraces are routinely neglected. It is not until recently that attention has begun to be paid to step fluctuations under nonequilibrium situations. In one such study by Uwaha and Saito [13], step roughness is examined by adding to the linear stability equation a hypothetical stochastic noise term representing the cumulative effect of all thermal fluctuations. The origin of their choice of the randomness, however, remains elusive. Another study, by Salditt and Spohn [14] on the time-dependent step roughness, took into account bulk random noise from the terraces but neglected noise contributions from excitations on the steps. Neither investigation considers multiple steps.

In this section, nonequilibrium step roughness is investigated using a Langevin formalism. Our approach is an extension of the general theoretical framework for the study of morphological fluctuations of solidification fronts at or near equilibrium, developed by Langer [15] and Karma [16], based on the procedures introduced by Cherepanova [17]. In this formalism, nonequilibrium, hydrodynamical fluctuations of the phase boundaries are evaluated as responses to the Langevin forces representing local thermodynamical fluctuations. We demonstrate that this Langevin formalism provides a consistent description of the kinetic roughness of steps. The effect of finite step spacing on step roughness, and the correlation between fluctuations on different steps, can all be conveniently evaluated. Our approach is limited in several aspects. The first and foremost limitation is related to the unresolved fundamental question of statistical mechanics of whether the Langevin formalism itself is applicable in treating statistical fluctuations of nonequilibrium systems. Second, our calculation is carried out in the small-amplitude limit and allows neither overhangs nor crossings of steps. Similarly, no interactions between steps beside the pure diffusive coupling is taken into account.

In the Langevin approach, stochastic noises are introduced to the diffusion equation and to the Gibbs-Thompson boundary condition as

$$\frac{\partial u(\mathbf{r},t)}{\partial t}=\nabla^2 u-u+q(\mathbf{r},t)\ , \tag{6.1}$$

$$u(x,\zeta^n,t)=\Delta-d_0\kappa\{\zeta^n\}-\beta v_n\{\zeta^n\}+\eta\{\zeta^n\}\ , \tag{6.2}$$

where the two independent Langevin forces q and η mimic fluctuations in adatom density on the terraces and near the steps, respectively. The noises are assumed to be Gaussian distributed with zero mean and variances

$$\langle q(\mathbf{r},t)q(\mathbf{r}',t')\rangle=2\Gamma(1-\nabla^2)\delta(\mathbf{r}-\mathbf{r}')\delta(t-t')\ , \tag{6.3}$$

$$\langle \eta(x,t)\eta(x',t')\rangle=2\beta\Gamma\delta(x-x')\delta(t-t')\ . \tag{6.4}$$

Note that the two-dimensionally distributed noise q comprises two contributions: one coming from the randomness in the impinging flux of atoms from the vapor, and the other from the adatom terrace diffusion processes itself. The magnitude Γ, as yet unspecified, will be fixed by the requirement that the method recovers correctly the equilibrium fluctuations.

Restricting ourselves to an infinite equidistant step train in the symmetric model, we write the stochastic equation of motion for the nth step as

$$\Delta-d_0\kappa-\beta v_n+\eta\{\zeta^n\}-\sigma(x,\zeta^n,t)=\sum_m\int dt_1dx_1G(x,\zeta^n,t|x_1,\zeta_1^m,t_1)\left[V+\frac{d\zeta_1^m}{dt_1}\right]\ , \tag{6.5}$$

where the two-dimensional noise is projected as

$$\sigma(x,\zeta^n,t)=\int dt_1d\mathbf{r}_1G(x,\zeta^n,t|\mathbf{r}_1,t_1)q(\mathbf{r}_1,t_1)\ . \tag{6.6}$$

Considering small-amplitude fluctuations around straight steps we linearize the above equation in the Fourier representation. The step profiles in response to the noises satisfy

$$\sum_{m=-\infty}^{+\infty}A_{n-m}(k,\omega)\hat{\zeta}^m(k,\omega)=\sigma^n(k,\omega)-\eta^n(k,\omega)\ , \tag{6.7}$$

where coefficients A_{n-m} only depend on the difference $n-m$:

$$A_0=\frac{1}{l}\left[\Delta+\frac{1}{e^{\alpha_+\lambda}-1}-\frac{1}{e^{\alpha_-\lambda}-1}-\frac{1}{Ml}\right]-i\omega\left[\frac{1}{2M}+\beta\right]-d_0k^2\ , \tag{6.8}$$

$$A_{n-m}=\begin{cases}-\left[\dfrac{i\omega}{2M}+\dfrac{1}{Ml^2}+\dfrac{1}{l}\right]e^{-(M+1/l)(n-m)\lambda}, & n>m\\ -\left[\dfrac{i\omega}{2M}+\dfrac{1}{Ml^2}-\dfrac{1}{l}\right]e^{(M-1/l)(n-m)\lambda}, & n<m\end{cases} \tag{6.9}$$

(6.10)

with $M(k,\omega)$ as previously defined. Also, we have

$$\sigma^n(k,\omega)=\int_{-\infty}^{+\infty}dz_1e^{-(z_1-n\lambda)/l-|z_1-n\lambda|M}\frac{q(k,\omega,z_1)}{2M(k,\omega)}\ . \tag{6.11}$$

The infinite set of equations (6.7) have the Toeplitz form and can be solved straightforwardly using Fourier series. Defining

$$\mathcal{A}(\theta)=\sum_{n=-\infty}^{\infty} A_n e^{in\theta},\quad Z(\theta)=\sum_{n=-\infty}^{\infty}\hat{\zeta}^n e^{in\theta}, \tag{6.12}$$

$$\mathcal{S}(\theta)=\sum_{n=-\infty}^{\infty}(\sigma^n-\eta^n)e^{in\theta}, \tag{6.13}$$

we have

$$\mathcal{A}(\theta)Z(\theta)=\mathcal{S}(\theta). \tag{6.14}$$

Inverting the Fourier series, we obtain

$$\hat{\zeta}^n(k,\omega)=\int_{-\pi}^{\pi}\frac{d\theta}{2\pi}\frac{\mathcal{S}(\theta)e^{-in\theta}}{\mathcal{A}(\theta)}, \tag{6.15}$$

which leads, noticing that $\langle\sigma^n\sigma^m\rangle$ only depends on $n-m$ and that $\langle\eta^n\eta^m\rangle=\langle\eta^0\eta^0\rangle\delta_{nm}$, to the result

$$\langle\hat{\zeta}^m(k\omega)\hat{\zeta}^0(k'\omega')\rangle=\int_{-\pi}^{\pi}\frac{d\theta}{2\pi}\frac{\langle\eta^0(k\omega)\eta^0(k'\omega')\rangle+\sum_n e^{in\theta}\langle\sigma^n(k\omega)\sigma^0(k'\omega')\rangle}{\mathcal{A}_{k\omega}(\theta)\mathcal{A}_{k'\omega'}(-\theta)}e^{-im\theta}. \tag{6.16}$$

This expression is the fluctuation spectrum for the infinite step train in response to stochastic noises from both the terraces and the steps. The stationary fluctuation spectrum can be evaluated from (6.16) by integrating out the arguments k', ω', and ω:

$$\langle\hat{\zeta}_k^m\hat{\zeta}_{-k}^0\rangle=\int\frac{d\omega d\omega' dk'}{(2\pi)^3}\langle\hat{\zeta}^m(k\omega)\hat{\zeta}^0(k'\omega')\rangle. \tag{6.17}$$

To proceed further with (6.16), we shall adopt the quasistatic approximation as before by neglecting the ω dependence in $M(k,\omega)$. Consequently, the noise correlators can be evaluated:

$$\langle\sigma^n(k\omega)\sigma^0(k'\omega')\rangle=\Gamma(2\pi)^2\delta(k+k')\delta(\omega+\omega')\times e^{-|n|\lambda M}\frac{1+\sinh(n\lambda/l)}{M}, \tag{6.18}$$

$$\langle\eta^0(k\omega)\eta^0(k'\omega')\rangle=2\beta\Gamma(2\pi)^2\delta(k+k')\delta(\omega+\omega'). \tag{6.19}$$

After some algebra, we find the general expression for the stationary fluctuation spectrum of steps

$$\langle\hat{\zeta}_k^m\hat{\zeta}_{-k}^0\rangle=\frac{\Gamma}{\pi}\int_{-\pi}^{\pi}\frac{d\theta e^{-im\theta}a(\theta)}{|b(\theta)c(-\theta)+b(-\theta)c(\theta)|}, \tag{6.20}$$

where

$$a(\theta)=2\beta M+\frac{\sinh M\lambda}{\cosh M\lambda-\cos\theta}, \tag{6.21}$$

$$b(\theta)=\frac{1}{l}\left[\Delta-d_0 lk^2+\frac{1}{e^{\alpha_+\lambda}-1}-\frac{1}{e^{\alpha_-\lambda}-1}-\frac{1}{Ml}\right]-\frac{1}{Ml^2}\left[\frac{1+Ml}{e^{(M+1/l)\lambda-i\theta}-1}+\frac{1-Ml}{e^{(M-1/l)\lambda+i\theta}-1}\right], \tag{6.22}$$

$$c(\theta)=1+2\beta M+\frac{1}{e^{(M+1/l)\lambda-i\theta}-1}+\frac{1}{e^{(M-1/l)\lambda+i\theta}-1}, \tag{6.23}$$

and the quasistatic $M=\sqrt{1+k^2+1/l^2}$. Equation (6.20) is the main result of this section.

First it is important to examine what (6.20) suggests about the equilibrium fluctuations. Setting $\Delta=0$, $l=\infty$, we have $a(\theta)=c(\theta)$, $b(\theta)=-d_0k^2$ and hence the equilibrium fluctuation spectrum

$$\langle\hat{\zeta}_k^m\hat{\zeta}_{-k}^0\rangle_{\rm eq}=\frac{\Gamma\delta_{m0}}{d_0k^2}. \tag{6.24}$$

We observe that the step roughness in equilibrium is independent of the step spacing λ. And apparently, in equilibrium, fluctuations on different steps also decouple since $\langle\hat{\zeta}_k^m\hat{\zeta}_{-k}^0\rangle_{\rm eq}=0$ and $m\neq0$.

Under nonequilibrium growth situations, however, fluctuations on different steps become correlated since in general $\langle\hat{\zeta}_k^m\hat{\zeta}_{-k}^0\rangle\neq0$ for $m\neq0$. Furthermore, Eq. (6.20) exhibits the familiar divergence of fluctuations at the onset of Mullins-Sekerka instability when $b(\theta=0)=0$. To see this more clearly, we consider the simple limit of a single step corresponding to $\lambda=\infty$. In this case the kinetic roughness spectrum of the step reduces to

$$\langle\hat{\zeta}_k^0\hat{\zeta}_{-k}^0\rangle=\frac{\Gamma}{|d_0k^2-\Delta/l+1/Ml^2|}, \tag{6.25}$$

where the denominator is proportional to the quasistatic dispersion relation of an isolated step. Extensions of the present calculation to include energetic interactions between steps and to incorporate asymmetric attachment kinetics may be warranted for direct comparison with experimental observations.

VII. COLLECTIVE MOTION OF STEPS —THE PHASE FIELD METHOD

A rich variety of collective behavior of steps is commonly encountered during changes of crystal surface topography. Steps are seldom uniformly spaced; pairwise grouping of steps, bunching of steps into macrosteps with height of multiple atomic units, collision and annihilation of step with antisteps, have all been observed in various surfaces of, for example, alkali halides [18], semiconductors [19], and metals [20]. To address these effects, fully time-dependent treatments of the collective movement of steps are necessary.

Theoretical analysis of the time-dependent multiple-step kinetics turns out to be formidable. The most well known continuum approach is the kinematic wave theory of Frank [21] using the method of characteristics [22]. Frank's theory treats bundles of steps as basic entities and monitors the temporal changes of the average step density. It does not trace the position of individual steps

and is therefore more coarse grained than the continuum BCF model. However, the method is found particularly useful in describing large scale changes of surface morphology involving macrosteps. Time evolution of step spacings in finite trains of steps has been discussed by Mullins and Hirth [23], based on the assumption that the step velocity is a function of only two adjacent step intervals. Both approaches apply to straight steps only and do not allow lateral variation of step profiles. Other time-dependent studies [24] of step motion either follow the spirit of Mullins and Hirth, or resort to explicit microscopic Monte Carlo simulations of the growth processes.

Meanwhile, the attempt towards a direct numerical solution of the original Stefan problem (2.5)–(2.7) is also difficult, hindered by the need to track explicitly all moving boundaries. This difficulty has highlighted in studies of dendritic solidification [7], and can be partly relieved using the so-called phase field method. It is the purpose of this section to develop a phase field model for the step problem. We shall demonstrate that this method provides a powerful tool permitting detailed study of time-dependent step kinetics.

The crux of the phase field approach [25] lies in the introduction of an order parameter $\phi(\mathbf{r},t)$ indicating the phase at a particular position. In our model, local stable minima of the order parameter correspond to terraces whereas rapid spatial variation of the order parameter locates the position of steps. Now we introduce a stochastic phase field model in the dimensionless form

$$\frac{\partial u(\mathbf{r},t)}{\partial t}=\nabla^2 u-u+\frac{1}{2}\frac{\partial \phi}{\partial t}+q(\mathbf{r},t)\ , \tag{7.1}$$

$$\tau\frac{\partial \phi(\mathbf{r},t)}{\partial t}=\xi^2\nabla^2\phi+a\sin(\pi\phi)-u+\Delta+q_\phi(\mathbf{r},t)\ , \tag{7.2}$$

where the last equation can be derived through a pure relaxational dynamics $\tau\partial\phi/\partial t=-\delta F/\delta\phi+q_\phi$ from the hypothetical free energy

$$F\{\phi,u\}=\int d^2\mathbf{r}\left[\frac{\xi^2}{2}(\nabla\phi)^2+\frac{a}{\pi}\cos(\pi\phi)+(u-\Delta)\phi\right]\ . \tag{7.3}$$

The Langevin noise q satisfies (6.3) while q_ϕ has zero mean and variance

$$\langle q_\phi(\mathbf{r},t)q_\phi(\mathbf{r}',t')\rangle=\frac{2\Gamma\xi^2}{\tau}\delta(\mathbf{r}-\mathbf{r}')\delta(t-t')\ . \tag{7.4}$$

The magnitude of variance is so chosen as to reproduce the correct interface noise η in the original sharp interface model discussed in the previous sections.

Equations (7.1) and (7.2) are extensions of the classical phase field model for solidification to the present problem with thermal fluctuations. A sinusoidal potential term is introduced to facilitate the description of multiple steps, by identifying the degenerate minima $\phi\sim(2i+1)\pi$, where i is an arbitrary integer, with terraces. The location of the moving steps is defined by the condition $\phi(\mathbf{r},t)=2i\pi$. The phase field model captures, phenomenologically, the effect of line tension and finite attachment kinetics by having finite values for ξ and τ, since ξ can be regarded as the thickness of steps and τ reflects the rate of response of the phase field. Parameter a is the strength of the potential which can be taken as a constant of order unity, when considering the limit of small supersaturations.

Formal methods have been used to establish the phase field model as a proper regularization of the original sharp interface problem (2.5)–(2.7). It has been shown [26], again formally using matched asymptotic expansions, that the phase field model recovers the sharp interface model by taking appropriate limits of quantities $\tau\to 0$, $\xi\to 0$, and $a\ll 1$. Following the standard procedures, it can be shown for our present model that the value of u at a step satisfies

$$u_{\text{step}}\approx\Delta-d_0\kappa-\beta v_n+\eta\ , \tag{7.5}$$

with the correspondences $d_0\sim\xi\sqrt{a}$, $\beta\sim\tau\sqrt{a}/\xi$, and that the projected Langevin noise η is governed by the correlator (6.4).

Equations (7.1) and (7.2), although stiff for small parameters ξ and τ, are suitable for direct numerical analysis [27]. While simulation on the physical two-dimensional geometry is straightforward, we focus here on the deterministic one-dimensional problem, corresponding to straight steps. First of all, numerical evidence suggests that (7.1) and (7.2) support steady state solutions with constant velocity, for infinite equidistant step trains with arbitrary spacing λ, and at all values of supersaturation $0<\Delta<1$. The most interesting application, however, concerns the time-dependent motion of finite, in general nonequidistant step trains. Such a situation is illustrated in Fig. 7, where a snapshot of the adatom density and order parameter profiles is displayed for a nonequidistant train of six steps. The parameters used in our numerical calculation are $\Delta=0.1$, $a=1$, $\tau=2.5\times10^{-3}$, $\xi=0.05$, and the average spacing between steps is $\lambda\approx2.5$. Strong overlap of the terrace diffusion fields is evident, even for average step spacing of $\lambda\approx2.5$. To dispel a reasonable misgiving, it is not hard to realize that an effective short-range repulsion exists between steps spaced on the scale of ξ. This conveniently avoids the possibility of steps behind overtaking others in the

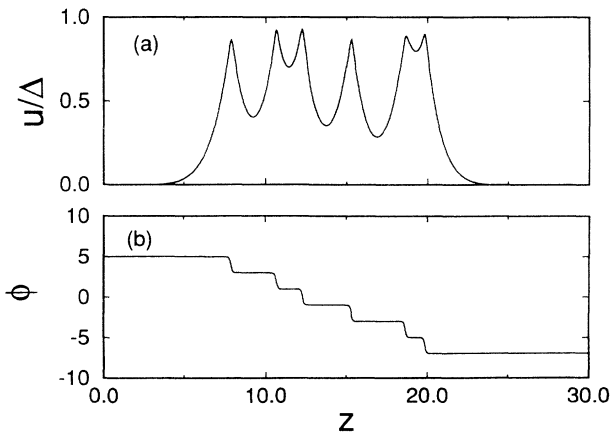

FIG. 7. Snapshot of (a) adatom density and (b) order parameter profiles, for a train of six steps. $\Delta=0.1$.

front, which in reality would create overhangs and involve prohibitive energy penalty.

A train of *finite* number of steps cannot propagate with equal spacing indefinitely, because there is no corresponding steady state solution. In Fig. 8, we consider the temporal evolution of a train of six steps starting from a configuration of equal step spacing $\lambda=0.5$ at $\Delta=0.1$. Step configurations at $t=0.5, 20, 60, 100, 140$ are shown in sequence. Both the leading step and the trailing step move faster than the steps inside the train, because each of them borders on an infinite terrace with richer adatom supply than other terraces. Therefore one expects the step train to pile up at the rear and spread at the front. This intuitive conclusion is indeed vividly observed in Fig. 8, where we see the bunching of the last three steps into a triple step, and the continuous breaking away of the leading steps from the train. Meanwhile, the overall extension of the step train increases monotonically in time. At $t=140$, the total length of the train has increased from an initial value of 3.0 to 16.14, by a factor of 5. It is also interesting to monitor the subsequent evolution of the triple step at the rear in Fig. 8. First it is clear that a step with multiple height moves much slower than the isolated steps. Consequently, the triple step lags farther behind the other steps until the leading step within the bunch finds a larger terrace in the front and accelerates to break away from the group. After a further dissociation of the remaining double step, the triple bunch eventually disassembles into elementary steps again. The qualitative conclusions we can now draw, that finite step trains are susceptible to bunching at the rear and spreading in the front, and that the average step density in a bunch decreases with time, are consistent with the analysis of Mullins and Hirth [23] and with the general results of Frank's kinematic wave theory [21].

In short we see that the complex dynamics of a finite step train result from the combined action of two effects—of step grouping from the rear and spreading from the front—each initiated from the two ends of the step train. Both effects can nevertheless be more instructively illustrated when examined separately, in Figs. 9 and 10. For instance, Fig. 9 shows the temporal development of pairwise bunching undulations on a semi-infinite step train. Clearly, the configuration of the step train at any time consists of a region with disturbances and an unperturbed region, separated by a propagating "shock" front. Within the region of disturbances, a pairwise bunching of steps occurs. In addition, the front appears to propagate uniformly with a constant velocity. A different behavior is observed for a moving semi-infinite step train which terminates on the right, as shown in Fig. 10. Here no bunching instability is present and the step train spreads smoothly. It is then inferrable from the foregoing discussions, confirmed by our numerical simu-

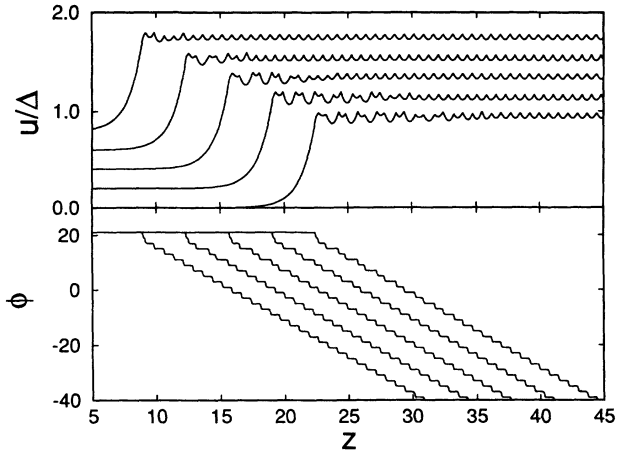

FIG. 9. Pairwise bunching of steps at the rear of a semi-infinite step train with uniform initial spacing $\lambda=0.75$ at $\Delta=0.2$. Curves from left to right are at $t=24$, 48, 72, 96, and 120. Adatom density profiles are vertically displaced by multiples of 0.2 to show clearly the propagation of bunching instability into the step train.

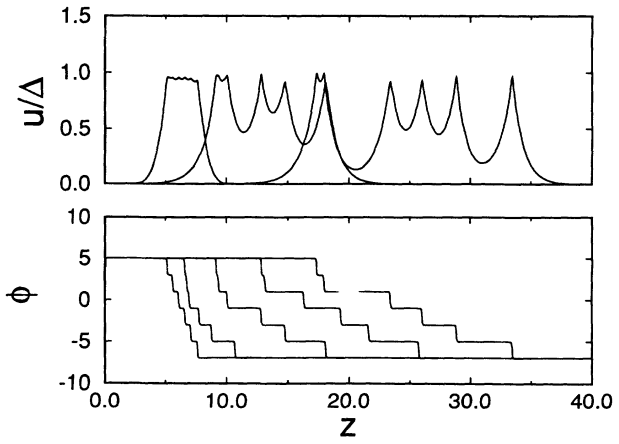

FIG. 8. Time evolution of a finite step train, starting from an initial configuration of six steps evenly spaced at $\lambda=0.5$. In the phase field (ϕ) plot, time sequences are, from left to right, $t=0.5$, 20, 60, 100, and 140. For clarity, only three instances of the diffusion field (u) at $t=0.5$, 60, and 140 are shown. $\Delta=0.1$.

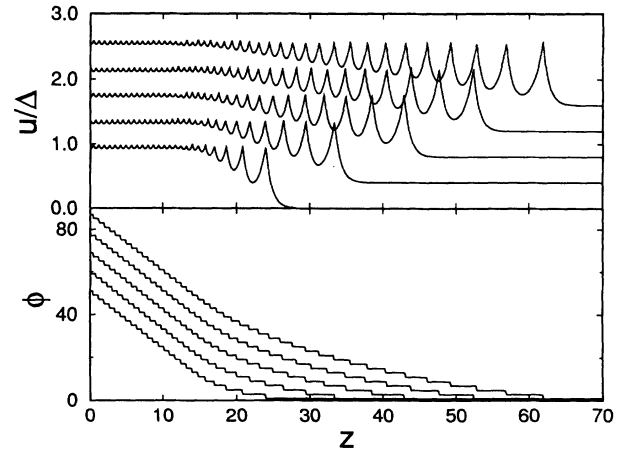

FIG. 10. Uniform spreading at the front of a semi-infinite step train with constant initial spacing $\lambda=0.75$ at $\Delta=0.2$. Step configurations from left to right correspond to $t=24$, 48, 72, 96, and 120. Adatom density profiles are vertically displaced by multiples of 0.4 for clarity.

lations, that whenever a large step train of lower step density invades that of a higher density, a shock front forms at the interface which propagates into the train of higher density and leaves behind a region of bunched step configurations. For a high density train running into a low density train, on the other hand, step spacings at the interface vary smoothly in space and interpolate between values characteristic of the two step trains.

These one-dimensional examples which we have hitherto considered are used to illustrate the utility of the phase field model to the study of microscopic kinetics of monoatomic steps. The major limitation of the present method lies in its difficulty in being generalized to the case of asymmetric step kinetics, due to the discontinuity in adatom density across the steps. Nevertheless, many physically important factors, such as the impurity obstruction to step motion, temporal changes of growth environment, spatial inhomogeneity in supersaturation, crystalline anisotropy, and the effect of island nucleation, can all be conveniently investigated using this phase field approach. Detailed studies of these aspects, in two dimensions, will be presented in the future.

ACKNOWLEDGMENTS

We are very grateful to James Langer for constant encouragements and for helpful suggestions. This work was supported in part by NSF Grant No. PHY89-04035, and the NSF Science and Technology Center for Quantized Electronic Structures (Grant No. DMR91-20007).

[1] W. K. Burton, N. Cabrera, and F. C. Frank, Philos. Trans. R. Soc. London, Ser. A **243**, 299 (1951).
[2] G. S. Bales and A. Zangwill, Phys. Rev. B **41**, 5500 (1990); **48**, 2024(E) (1993).
[3] R. Ghez and S. S. Iyer, IBM J. Res. Dev. **32**, 804 (1988).
[4] R. Ghez, H. G. Cohen, and J. B. Keller, Appl. Phys. Lett. **56**, 1977 (1990).
[5] D. G. Vlachos and K. F. Jensen, Surf. Sci. **262**, 359 (1992).
[6] R. L. Schwoebel and E. J. Shipsey, J. Appl. Phys. **37**, 3682 (1966); R. L. Schwoebel, *ibid.* **40**, 614 (1969).
[7] J. S. Langer, Rev. Mod. Phys. **50**, 1 (1980); N. D. Goldenfeld, in *Metastability and Incompletely Posed Problems,* edited by S. Antman *et al.* (Springer-Verlag, Berlin, 1987); D. A. Kessler, J. Koplik, and H. Levine, Adv. Phys. **34**, 123 (1990).
[8] J. S. Langer and L. A. Turski, Acta Metall. **25**, 1113 (1977); J. S. Langer, *ibid.* **25**, 1121 (1977).
[9] W. W. Mullins and R. F. Sekerka, J. Appl. Phys. **34**, 323 (1963); **35**, 444 (1964).
[10] C. Misbah and W. Rappel, Phys. Rev. B **48**, 12 193 (1993).
[11] P. Bennema and G. H. Gilmer, in *Crystal Growth: An Introduction,* edited by P. Hartman (North-Holland, Amsterdam, 1973).
[12] Equilibrium properties of steps are recently reviewed in E. D. Williams and N. C. Bartelt, Science **251**, 393 (1991).
[13] M. Uwaha and Y. Saito, Phys. Rev. Lett. **68**, 224 (1992); Surf. Sci. **283**, 366 (1993).
[14] T. Salditt and H. Spohn, Phys. Rev. E **47**, 3524 (1993).
[15] J. S. Langer, Phys. Rev. A **36**, 3350 (1987); J. A. Warren and J. S. Langer, Phys. Rev. E **47**, 2702 (1993).
[16] A. Karma, Phys. Rev. Lett. **70**, 3439 (1993); Phys. Rev. E **48**, 3441 (1993).
[17] T. A. Cherepanova, Dokl. Akad. Nauk SSSR **226**, 1066 (1976) [Sov. Phys. Dokl. **21**, 109 (1976)].
[18] K. W. Keller, Metall. Trans. **22A**, 1299 (1991); H. Bethge *et al.*, J. Cryst. Growth **48**, 9 (1980).
[19] A. V. Latyshev *et al.*, Surf. Sci. **213**, 157 (1989); A. V. Latyshev, A. B. Krasilnikov, and A. L. Aseev, Appl. Surf. Sci. **60**, 397 (1992); E. Bauser and H. Struck, Thin Solid Films **93**, 185 (1982).
[20] T. Hsu, Ultramicroscopy **11**, 167 (1983); S. Ogava *et al.*, J. Vac. Sci. Technol. **5**, 1735 (1987).
[21] F. C. Frank, in *Growth and Perfection of Crystals,* edited by R. H. Doremus, B. W. Roberts, and D. Turnbull (Wiley, New York, 1958); N. Cabrera and D. A. Vermilyea, *ibid.*; A. A. Chernov, Usp. Fiz. Nauk **73**, 277 (1961) [Sov. Phys. Usp. **4**, 116 (1961)].
[22] On the application of the method of characteristics to crystal growth, see J. E. Taylor, J. W. Cahn, and C. A. Handwerker, Acta Metall. Mater. **40**, 1443 (1992).
[23] W. W. Mullins and J. P. Hirth, J. Phys. Chem. Solids **24**, 1391 (1963).
[24] For example, D. Kandel and J. D. Weeks, Phys. Rev. Lett. **69**, 3758 (1992); R. van Rosmalen and P. Bennema, J. Cryst. Growth **32**, 293 (1976); C. van Leeuwen, R. van Rosmalen, and P. Bennema, Surf. Sci. **44**, 213 (1974).
[25] The idea of phase field approach in the crystal growth context was put forward by many authors, for example, G. Fix, in *Free Boundary Problems,* edited by A. Fasano and M. Primicerio (Pittman, London, 1983); J. B. Collins and H. Levine, Phys. Rev. B **31**, 6119 (1985); J. S. Langer, in *Directions in Condensed Matter Physics,* edited by G. Grinstein and G. Mazenko (World Scientific, Singapore, 1986).
[26] G. Caginalp, Phys. Rev. A **39**, 5887 (1989); a different formal procedure is carried out by R. Kupferman, O. Shochet, E. Ben-Jacob, and Z. Schuss, Phys. Rev. B **46**, 16 045 (1992).
[27] For a more sophisticated numerical scheme for one-dimensional phase field models, see H. Lowen, J. Bechhoefer, and L. S. Tuckerman, Phys. Rev. A **45**, 2399 (1992).